Trehalose delays postmenopausal osteoporosis by enhancing AKT/TFEB pathway-dependent autophagy flow in rats

YONGLI WANG[1*], XINGCUN LI[2*], HONGLIANG GAO[1] and QIAN LU[1]

[1]Department of Orthopedics and [2]Public Health Section, Huzhou Central Hospital, Huzhou Basic and Clinical Translation of Orthopedics Key Laboratory, Huzhou, Zhejiang 313300, P.R. China

Abstract. Osteoporosis is a systemic bone metabolic disorder that plagues the health and quality of life of the elderly. Autophagy plays an important role in bone formation while maintaining the homeostasis of the body. Trehalose is a mTOR-independent autophagy inducer, but to the best of our knowledge, there is no rat model of postmenopausal osteoporosis. The present study found that trehalose can delay postmenopausal osteoporosis in rats, which may be achieved by inducing and enhancing AKT/transcription factor EB pathway-dependent autophagy flow. The specific mechanism of its occurrence needs to be further studied. Trehalose-containing drugs are promising for delaying postmenopausal osteoporosis. Hematoxylin and eosin (H&E) staining, western blotting, micro computerized tomography (CT) scanning and Transmission electron microscopy were used to investigate the role of trehalose in postmenopausal osteoporosis rat model at protein, cell and histology aspects. According to the H&E staining results, the bone trabecular histological structure of the trehalose group was superior to that of the model group. The Micro CT scanning indicated the imaging structure of bone trabeculae in the trehalose group was superior to than that in the model group. Western blotting indicated the activation of autophagic flow in trehalose group, the autophagy degree of the trehalose group is greater than that of the model group; Transmission electron microscopy indicated the autophagy degree of the Trehalose group was greater than that of the model group under electron microscopy. Trehalose can delay postmenopausal osteoporosis in rats, which may be achieved by inducing and enhancing Akt/TFEB pathway-dependent autophagy flow.

Correspondence to: Dr Qian Lu or Mr. Hongliang Gao, Department of Orthopedics, Huzhou Central Hospital, Huzhou Basic and Clinical Translation of Orthopedics Key Laboratory, 1558 North Third Ring Road, Wuxing, Huzhou, Zhejiang 313300, P.R. China
E-mail: yongliw@yeah.net
E-mail: hzsgkjcylczhzdsys@163.com

*Contributed equally

Introduction

Osteoporosis is a systemic bone metabolic disorder characterized by the destruction of bone tissue microstructure, the continuous reduction of the proportion of bone mineral composition and bone matrix proportion, bone thinning, reduction of the number of bone trabeculae, increased bone fragility and increased risk of fracture (1). According to the relevant statistical data of WHO, the incidence rate of osteoporosis has been increasing yearly. Osteoporosis is responsible for 8.9 million fractures each year. It is estimated that by 2050, the global number of hip fracture patients induced by osteoporosis will increase by 310% in men and 240% in women, especially in postmenopausal women (2). In China, the prevalence rate of osteoporosis in women >50 years old was 32.1% and that in females >65 years old was 51.6%,with the incidence of complicated fractures ~33% (1-4). With increasing aging globally, osteoporosis has become a major disease that affects the health and quality of life of the elderly, especially in postmenopausal women. Therefore, the pathogenesis and prevention methods of postmenopausal osteoporosis have been the focus of academic research.

Autophagy is a phenomenon that widely exists in eukaryotic cells to maintain self-stability. In addition to maintaining self-protection for emergency factors (5), it also plays an important role in bone formation (6-8). Researchers have found that trehalose is a mTOR-independent autophagy inducer, which can promote the degradation of toxic proteins in cells (9). In addition, trehalose has been approved for human use by the US Food and Drug Administration as safe and harmless to human body and has broad clinical application prospects.

There have been no studies, to the best of our knowledge, on the effect of trehalose on postmenopausal osteoporosis. Our research team found that trehalose can delay the development of postmenopausal osteoporosis in previous studies (10,11), but its mechanism is still unclear. The present study further investigated whether trehalose delay postmenopausal osteoporosis by enhancing AKT/transcription factor EB (TFEB) pathway-dependent autophagy.

Materials and methods

Laboratory animals and modeling. The present study was approved by the Institutional Animal Care and Use Committee

of Hangzhou Hibio Animal Care Technology Co., Ltd. (IACUC protocol number HBFM 3.68-2015) and the animal experiments were performed at Hangzhou Hibio Animal Care Technology Co., Ltd.

A total of 18 healthy female SD rats, each weighing 200 g and aged 6 weeks, were purchased from Shanghai Slake Laboratory Animal Co., Ltd. Experimental animals received *ad libitum* feed and water and 12/12-h of daily light/dark time. The rats were SPF grade the supplier held license number SCXK (Shanghai) 20170005 and certificate number 20170005021392. The drinking water was sterilized Grade II ultrapure water and the quality of drinking water complied with the national standard of the People's Republic of China, Hygienic Standard for Drinking Water (GB5749 2006). The laboratory animal room is licensed under SYXK (Zhe) 2015 0008, with a breeding environment featuring a temperature range of 20-25°C and relative humidity range of 40-70%. Prior to experimentation, the animals were acclimated to the animal room environment for one week.

After adaptive feeding, the 18 rats were randomly assigned to three groups: Normal group (n=6), model group (n=6) and trehalose group (n=6). Following one week of adaptation, each rat in the model and trehalose groups underwent anesthesia with a 2% (w/v) pentobarbital sodium solution administered via intraperitoneal injection. The abdominal hair of the rats was removed using a depilatory agent and disinfected as per standard protocol. The rats in the model group underwent a 1-2 cm incision in the abdomen to expose the uterus, which was ligated, and the ovaries removed followed by closure of the abdominal cavity. The normal group were subjected to identical procedures without additional ligation and ovariectomy. All rats were administered penicillin injections for three consecutive days. At the 16-week modeling mark, the trehalose group was administered gavage of 100 mg/kg trehalose with a volume of 0.2 ml/10 g, (12,13), while an equivalent volume of drinking water was given to the model and normal group. The normal group received no treatment. After 16 weeks, both groups were sacrificed using a massive intraperitoneal injection of 2% (w/v) pentobarbital sodium solution and their femurs on both sides were extracted. One side was frozen, the other side was fixed in 4% paraformaldehyde solution at room temperature for 24 h and then treated with decalcifying solution for 2 month at 37°C.

Hematoxylin and eosin (H&E) staining. Tissue sections were subjected to H&E staining in room temperature. The paraffin sections were melted in an oven at 65°C for ~45 min, followed by two rounds of dewaxing with xylene for ~10 min each time. Then, they were hydrated using a gradient ethanol series (100, 90, 80, and 70% ethanol) and washed with PBS before being immersed in hematoxylin solution for five minutes. After rinsing with running water, the sections underwent acidic differentiation and eosin staining before weak acid differentiation and another rinse. Finally, the stained tissue sections were dehydrated using ascending ethanol solutions starting from low concentration to higher concentrations before sealing.

Western blotting. Protein was extracted from tissue using tissue lysis buffer (Beyotime Institute of Biotechnoloy;

cat. no. P0013B) for 1 h and centrifuge (12,000 x g, 15 min, 4°C) to obtain the supernatant. s to use the BCA reagent kit (Beyotime, P0009) to determine protein concentration. The 10% SDS-PAGE precast gel solution (Beyotime Institute of Biotechnology) was prepared according to the manufacturer's instructions and added between two glass plates. The electrophoresis buffer was formulated by adding glycine (Beyotime, ST085), Tris (Beyotime, ST760-500 g) and SDS (Beyotime Institute of Biotechnology; cat. no. ST627) in specific proportions to ultrapure water while membrane transfer buffer was made by mixing glycine, Tris, SDS and methanol in certain ratios. The SDS-PAGE gel plate was secured onto the electrophoresis clamp, followed by removal of the loading comb and addition of 15 μl cell protein and 10 μl tissue protein per well, along with 2 μl protein ladder at both ends. The electrophoresis process was initiated by accurately positioning the electrodes and introducing a preconfigured electrophoresis solution. The electrophoresis was conducted under a constant voltage regime, whereby the protein sample was subjected to 80 V until it migrated beyond the separation gel and subsequently at 120 V for 55 min. The separation of proteins with varying molecular weights was achieved through differential migration in response to an electric field. Electrophoresis could be terminated once the target molecular weights were adequately resolved and membrane transfer using a 0.22 μm pore size PVDF membrane for wet transfer printing was performed. The entire membrane was placed into the groove and immersed in liquid to initiate film transfer. The membrane transfer was performed at 300 mA for about 90-120 min. The specific transfer time should be adjusted according to the molecular weight of the target protein and the time needed for the larger molecular weight was longer. The protein containing membrane was blocked with 5% BSA (cat. no. ST023-50 g; Beyotime Institute of Biotechnology) solution for 2 h at room temperature and then washed with TBST solution (5 min, 3 times; 0.1% Tween). Target molecular weight bands were excised, with reference to the protein ladder on both sides. The bands were incubated with preconfigured primary antibodies against the target protein for 12-16 h on a shaker at 4°C. The primary antibodies used were AKT (1:1,000; Cell Signaling Technology, Inc.; cat. no. 9272S), phosphorylated (p-)AKT (1:1,000; Cell Signaling Technology, Inc.; cat. no. 4060S), TFEB (1:1,000; BIOSS; cat. no. bs5137R), GAPDH (1:2,000, Multi Sciences cat. no. Mab5465 100), LC3 (1:1,000; Abcam; cat. no. ab62721) and P62 (1:1,000; Abcam; cat. no. ab109012). Cells underwent three washes with TBST solution (5 min each) and were subsequently co-incubated with secondary antibody solution of identical species origin for 2 h. The secondary antibodies were horseradish peroxidase-conjugated goat anti-rabbit IgG (1:5,000; Beyotime Institute of Biotechnology; cat. no. A0208) and Goat anti Mouse IgG (1:5,000; Beyotime Institute of Biotechnology; cat. no. A0216). BeyoECL Plus (cat. P0018M, Beyotime) was used to bind secondary antibodies for chemiluminescence. Upon conclusion of incubation, the bands received an additional three washes in similar fashion. Chemiluminescence imaging system was used for image acquisition and subsequent analysis.

Micro computerized tomography (CT) scanning. The frozen femur tissue were harvested and fixed in 4% paraformaldehyde
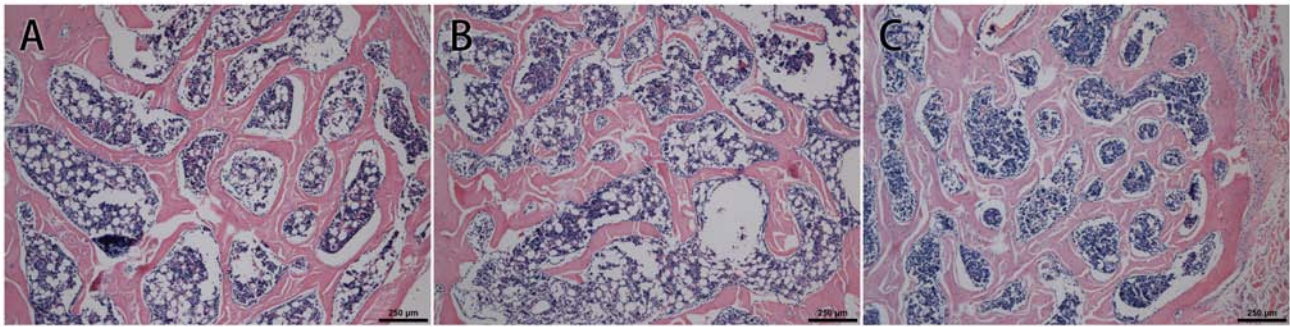
Figure 1. At 16 weeks after modeling, the hematoxylin and eosin staining of femoral sections in three groups, the bone trabeculae in the (A) trehalose group are thicker than those in (B) model group and smaller than (C) normal group.

for 48 h at room temperature. Subsequently, the prepared femur was subjected to Micro CT scanning using a source voltage of 70 KV and current of 200 μA with exposure time of 300 msec and resolution of 10 μm. The images were reconstructed into a three-dimensional model using SCANCO MICROCT Evaluation V6.5-3 (SCANCO Medical AG) analysis software, from which regions of interest were selected for quantitative analysis. The specific analysis indices were as follows: scanning bone volume (TV) was expressed in cubic millimeters, bone volume (BV) in the region of interest (ROI) was expressed in cubic millimeters, bone volume fraction (BV/TV) was expressed as a percentage, trabecular thickness (Tb. Th) was expressed in μm, number of bone trabeculae (Tb. N) was expressed per mm and separation degree of bone trabeculae (Tb. SP), represented by bone mineral density (BMD), was expressed in m g/cm^3.

Transmission electron microscopy. Femoral tissue (<1 mm^3) excised following euthanasia were fixed overnight in 2.5% glutaraldehyde PBS (12 h at room temperature); flushed with 0.1 M PBS for 15 min, 2 times; fixed with 1% osmic acid for 1 h at 37˚C, washed with 0.1 M PBS for 15 min, 2 times; stained with 2% uranium acetate solution for 30 min at room temperature; dehydrated with 50, 70 and 90% alcohol successively for 15 min; dehydrated with 100% alcohol for 20 min; dehydrated with 100% acetone for 20 min, 2 times; anhydrous acetone and embedding agent were mixed in 1:1 volume to penetrate the tissue and vibrated for 2 h at room temperature; pure embedding agent and vibrated for 2 h at room temperature. Finally, the tissue blocks were embedded with pure embedding agent which was polymerized in the oven at 37˚C for 24 h, 45˚C for 24 h and 60˚C for 48 h. The block was trimmed and sectioned at ~120 nm. Staining was performed with 4% uranium acetate for 20 min and lead citrate for 5 min at room temperature. The stained ultrathin section were placed on single hole copper mesh and observation and images were captured using a transmission electron microscope (TECNAI-10, 80 kV, Philips, magnification, x2,500 times). Digital micrograph 3.4 (Gatan, America) was used for analysis.

Statistical analysis. The data are presented as mean ± standard deviation and statistical analysis was performed using SPSS 20.0 (IBM Corp.). The significance of differences between two groups was determined by two-tailed unpaired Student's t-test using GraphPad Prism 8 software (GraphPad Software Inc.; Dotmatics). One-way ANOVA was used to determine significant differences among the three groups. P<0.05 was considered statistically significant.

Results

H&E staining. According to the H&E staining results, the bone trabeculae and hematopoietic tissue in the bone marrow cavity of the femur in the normal group were evenly distributed, while the bone trabeculae in the model group and trehalose group were small and dense. The bone trabeculae in the model group were narrower than those in the trehalose group. These results indicated that the bone trabecular histological structure of the trehalose group was superior to that of the model group (Fig. 1).

Micro CT scanning. Compared with the normal group, BV/TV, BMD, Tb. N and Tb. Th in the model group decreased and trabecular separation Tb. SP increased, with statistically significant differences (P<0.05); Compared with the model group, the trehalose group had higher BV/TV, BMD, Tb. N, Tb. Th and decreased Tb. SP, with statistically significant differences (P<0.05). These results indicated that the imaging structure of bone trabeculae in the trehalose group was superior to than that in the model group (Table I).

Western blotting. Compared with the normal group, the expression of TFEB and LC3 protein in the model group was upregulated, while the expression of p-AKT and P62 protein was down regulated and there was a significant difference (P<0.05). Compared with the model group, the expression of TFEB and LC3 protein in trehalose group was upregulated, while the expression of p-AKT, p-AKT/AKT ratio and P62 protein was downregulated and there was a significant difference (P<0.05); There was no significant change in AKT protein expression in each group (P>0.05). These results indicated the activation of autophagic flow in trehalose group, the autophagy degree of the trehalose group is greater than that of the model group (Fig. 2).

Transmission electron microscopy. At the 16th week of modeling, the number of autophagosomes in trehalose group was the largest among the three groups. The results of transmission electron microscopy showed that the number of

Table I. Quantitative morphometric parameters of micro computerized tomography of distal femur.

Group	BV/TV(%)	Tb. Th (μm)	Tb. N	BMD (mg/cm^3)	Tb. Sp (μm)
Normal group	0.276±0.034	0.076±0.005	3.898±0.336	909.886±10.302	0.170±0.017
Model group	0.190±0.014	0.048±0.013	2.503±0.326	869.668±22.589	0.277±0.020
Trehalose group	0.234±0.023	0.068±0.001	3.251±0.222	882.979±12.003	0.234±0.018

BV/TV vs. the normal group (group 1 for short), the model group (group 2 for short) and trehalose group (group 3 for short) decreased: $P_{12}\approx0.005$, $P_{23}\approx0.07$, $P_{13}\approx0.08$. Tb. Th vs. the normal group, it decreased in the model group and trehalose group ($P_{12}\approx0.005$, $P_{23}\approx0.02$, $P_{13}\approx0.27$). Tb. N vs. the normal group, it decreased in the model group and trehalose group ($P_{12}\approx0.001$, $P_{23}\approx0.02$, $P_{13}\approx0.04$); BMD vs. the normal group, BMD in model group and trehalose group decreased ($P_{12}\approx0.02$, $P_{23}\approx0.04$, $P_{13}\approx0.35$); Tb. Sp vs. the normal group, it increased in the model group and trehalose group ($P_{12}\approx0.0004$, $P_{23}\approx0.03$, $P_{13}\approx0.005$).
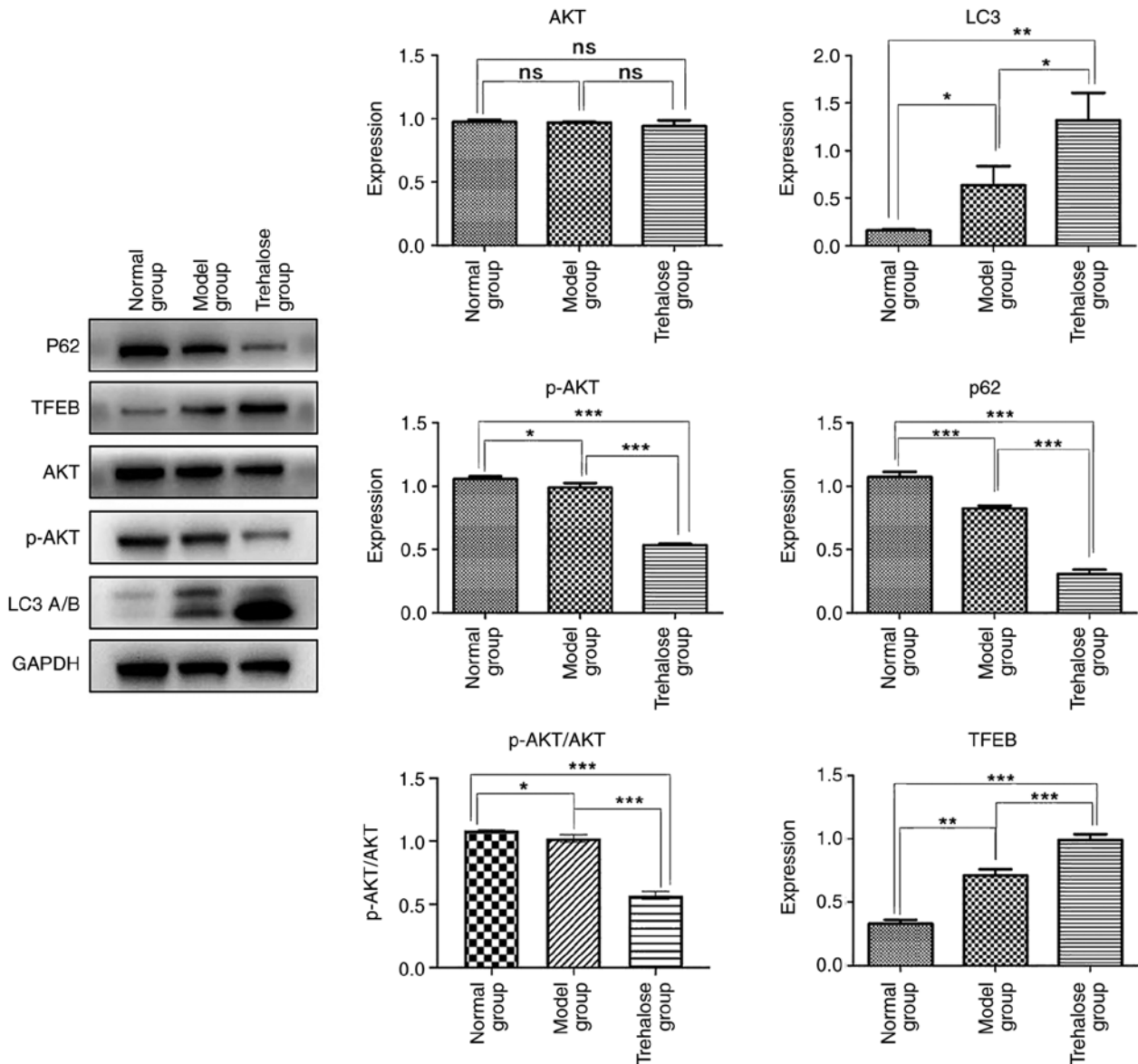

Figure 2. Expression of p-AKT, LC3, TFEB, p62 and AKT proteins in three groups detected by western blotting. The expression of TFEB and LC3 protein in the model group was up regulated, while the expression of p-AKT, p-AKT/AKT ratio and P62 protein was downregulated and there was a significant difference (P<0.05); there was no significant change in AKT protein expression in each group (P>0.05). The data represent means ± SD; *P<0.05, **P<0.01 and ***P<0.001. ns, not significant; p-, phosphorylated; TFEB, transcription factor EB.

autophagosomes was trehalose group>model group>normal group. These results indicated the autophagy degree of the Trehalose group was greater than that of the model group under electron microscopy (Fig. 3).
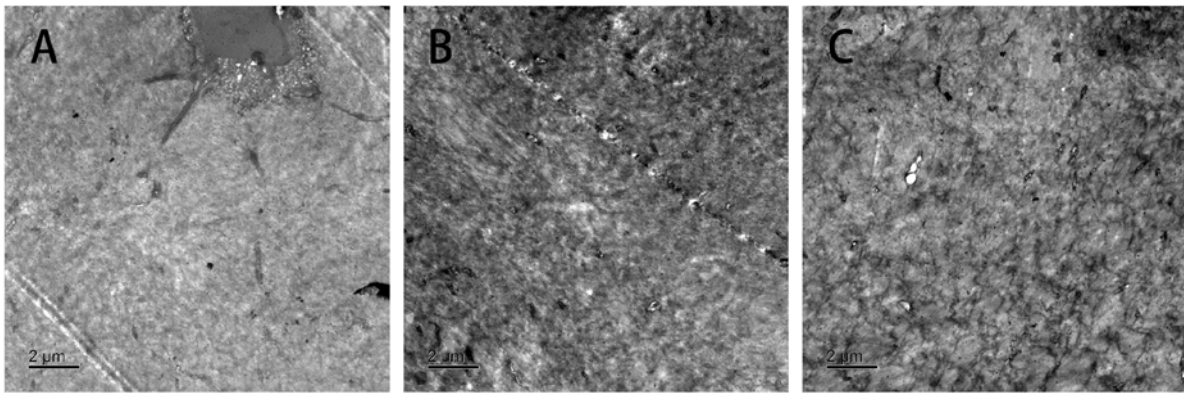
Figure 3. At 16 weeks after modeling, transmission electron microscope examination of the three groups. The ranking of the number of autophages was (A) normal group< (B) model group< (C) trehalose group. White arrows indicate autophagosomes.

Discussion

Osteoporosis is a systemic osteopathy characterized by low bone mass, destruction of bone tissue microstructure, increased bone fragility and ease of fracture. With the aging of the population, osteoporosis has become an important public health problem in China. An epidemiological survey showed that the prevalence of osteoporosis in the population >50 years old in China was 20.7%, especially in postmenopausal women (4). Osteoporosis is preventable and curable (1). The research on the pathogenesis and prevention methods of osteoporosis has been a hot topic in the academic community.

Autophagy is a phenomenon that widely exists in eukaryotic cells to maintain homeostasis. Stimulated by some factors (including ischemia, hypoxia and starvation), autophagy precursor forms an autophagic vesicle with double membrane structure, which gradually encapsulates proteins and organelles to be degraded, forming autophagolysosome and then the outer membrane of autophagolysosome fuses with lysosomes to form an autolysosome, which then enter the lysosome cavity and is degraded by proteolytic enzymes. The degraded components are recycled by cells (14). The process of autophagy *in vivo* includes three steps: Autophagosome formation, autolysosome fusion and autolysosome degradation. The dynamic process of each step is called autophagy flow (15). The potential regulatory mechanism of autophagy flow is a post transcriptional regulation. As a member of the microphthalmia/translation Factor E (MiTF/TFE) family of leucine zipper basic helix loop helix-leucine zipper (bHLH-LZ) transcription factors, TFEB plays an important role in regulating a variety of cellular processes (16,17). The transcriptional activity of TFEB is mainly regulated by two pathways, namely serine/threonine protein kinase AKT and mTOR1. AKT and mTOR1 phosphorylate TFEB filament amino acid 467 (Ser467) and 211 (Ser211), respectively, to make TFEB form a complex and remain in the cytoplasm. Once AKT and mTOR are inactivated under the action of their respective inhibitors, TFEB complex can be disassembled and free TFEB enters the nucleus, exerting its transcription factor effect and finally achieving the effect of enhanced autophagic flow.

In previous studies (10,18,19), it was found that trehalose has the biological activity of inhibiting AKT and can induce TFEB phosphorylation and nuclear internalization downstream
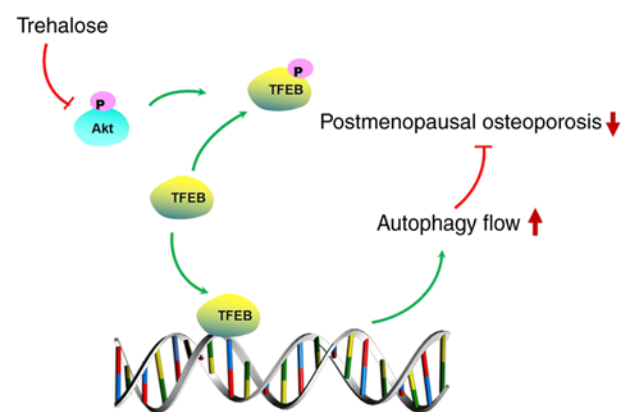

Figure 4. The scheme of trehalose regulating autophagic flow to delay postmenopausal osteoporosis. the trehalose promoted the TFEB-mediated autophagic flow to delay postmenopausal osteoporosis. p, phosphorylation; TFEB, transcription factor EB.

of AKT, thus leading to the enhancement of autophagic flow in cells (18). Nishizaki *et al* (17) and Yoshizane *et al* (18) studied the changes of osteoclast in ovariectomized mice after trehalose use and proved that trehalose could inhibit the activation of osteoclast by decreasing IL-6 and TNF-α, and that trehalose could inhibit bone loss. However, ovariectomy results in cancellous osteopenia and accelerated bone turnover in the mice. There are differences between human and mice physiology regarding the actions of estrogens and estrogen analogs such as tamoxifen. While these species differences do not necessarily contraindicate its use, the ovariectomized mice model should be approached with extreme caution (19). Therefore, the rat model is a more ideal model than a mice model for studying postmenopausal osteoporosis. Also, Nishizaki *et al* (17) and Yoshizane *et al* (18) 20 years ago had performed relatively simple researches on the changes of osteoclast under the trehalose use and no further research on the mechanism. Xu *et al* (20) showed that trehalose decreased the OB-mediated osteoclastogenesis and reduced the primary biliary cirrhosis (PBC)-related bone loss by regulating ERK phosphorylation via autophagosome formation, proving the potential value of trehalose in delaying osteoporosis as have we (20). However, they studied bile duct-ligated male rats which belonging to a secondary osteoporosis model. Bone loss

was just a severe complication of PBC and their model could not be used for postmenopausal osteoporosis. This is why the present study chose the trehalose for further research.

In the present study, compared with the model group, the trehalose group decreased the expression of p-AKT and P62 protein and increased the expression of LC3 and TFEB protein, suggesting that the trehalose induced increase in TFEB expression and autophagy level. At the same time, via histology, the trabecular arrangement in trehalose group was more dense and uniform than that in model group at 16 weeks, with less change. Micro CT showed that the trabecular bone number, trabecular structure arrangement, trabecular bone space and separation in trehalose group were improved compared with than those in model group at 16 weeks of modeling; In transmission electron microscopy, autophagosome had three forms according to the different stages of autophagy. In the early stage, it was shaped like crescent and wrapped around the cytoplasmic components; In the middle stage, it had a bilayer or multilayered vacuole structure, containing cytoplasm and organelles such as ribosome or mitochondria; in the later stage, it had a single-layer membrane structure and the internal slurry composition had been degraded (21). The increase of autophagosomes indicated an increase in autophagosome synthesis or inhibition of autolysosome fusion, so it was necessary to exclude the situation of blocked autolysosome fusion by detecting the P62 expression.

In Fig. 3, the number of autophagosomes in the trehalose group was greater than that in other groups. The number of autophagosomes of the trehalose group mainly manifested as vacuoles or containing contents, similar to the morphology of autophagosomes in the middle and late stages, combined with the expression of autophagy digestion substrate P62, indicating enhanced autophagy in the trehalose group. Based on the results of the present study, it is hypothesized that after the use of trehalose, p-AKT in rat bone tissue is inhibited and downregulated, promoting the dissociation of TFEB complex, TFEB nuclear translocation and enhancing autophagic flow, leading to an increase in LC3 expression and a decrease in P62 expression, finally alleviating postmenopausal osteoporosis (Fig. 4).

However, there are still some limitations to the present study. First, the postmenopausal rat model was used in the experiment and no relevant experiments were performed on other animals. Second, *in vitro* experiments were not performed; In addition, the effect of trehalose on AKT/TFEB pathway dependent autophagy flow was only preliminarily discussed, but the specific mechanism and the relationship between trehalose and osteoporosis need to be further explored.

Trehalose can delay postmenopausal osteoporosis in rats, which may be achieved by inducing and enhancing AKT/TFEB pathway-dependent autophagy flow. The specific mechanism of its occurrence remains to be studied. Trehalose-containing drugs have prospects in delaying postmenopausal osteoporosis.

Availability of data and materials

The datasets used and/or analyzed during the current study are available from the corresponding author on reasonable request.

Authors' contributions

QL conceived the present study. HG constructed figures and contributed to the analysis and interpretation of data. XL and YW designed the study and wrote the manuscript. QL and YW revised the manuscript. All authors read and approved the final manuscript. YW and QL confirm the authenticity of all the raw data.

Ethics approval and consent to participate

The present study was approved by the Institutional Animal Care and Use Committee of Hangzhou Hibio Animal Care Technology Co., Ltd. (IACUC protocol number HBFM 3.68-2015) and the animal experiments were carried out at Hangzhou Hibio Animal Care Technology Co., Ltd.

Patient consent for publication

Not applicable.

Competing interests

The authors declare that they have no competing interests.

References

1. Arceo-Mendoza RM and Camacho PM: Postmenopausal osteoporosis: Latest guidelines. Endocrinol Metab Clin North Am 50: 167-178, 2021.
2. Gopinath V: Osteoporosis. Med Clin North Am 107: 213-225, 2023.
3. Ayers C, Kansagara D, Lazur B, Fu R, Kwon A and Harrod C: Effectiveness and safety of treatments to prevent fractures in people with low bone mass or primary osteoporosis: A living systematic review and network meta-analysis for the American college of physicians. Ann Intern Med 176: 182-195, 2023.
4. Zhang C, Feng J, Wang S, Gao P, Xu L, Zhu J, Jia J, Liu L, Liu G, Wang J, *et al*: Incidence of and trends in hip fracture among adults in urban China: A nationwide retrospective cohort study. PLoS Med 17: e1003180, 2020.
5. Galluzzi L, Pietrocola F, Levine B and Kroemer G: Metabolic control of autophagy. Cell 159: 1263-1276, 2014.
6. Nuschke A, Rodrigues M, Stolz DB, Chu CT, Griffith L and Wells A: Human mesenchymal stem cells/multipotent stromal cells consume accumulated autophagosomes early in differentiation. Stem Cell Res Ther 5: 140, 2014.
7. Whitehouse CA, Waters S, Marchbank K, Horner A, McGowan NW, Jovanovic JV, Xavier GM, Kashima TG, Cobourne MT, Richards GO, *et al*: Neighbor of Brca1 gene (Nbr1) functions as a negative regulator of postnatal osteoblastic bone formation and p38 MAPK activity. Proc Natl Acad Sci USA 107: 12913-12918, 2010.

8. Chang KH, Sengupta A, Nayak RC, Duran A, Lee SJ, Pratt RG, Wellendorf AM, Hill SE, Watkins M, Gonzalez-Nieto D, *et al*: p62 is required for stem cell/progenitor retention through inhibition of IKK/NF-kappaB/Ccl4 signaling at the bone marrow macrophage-osteoblast niche. Cell Rep 9: 2084-2097, 2014.

9. He Q, Koprich JB, Wang Y, Yu WB, Xiao BG, Brotchie JM and Wang J: Treatment with trehalose prevents behavioral and neurochemical deficits produced in an AAV α-Synuclein rat model of Parkinson's disease. Mol Neurobiol 53: 2258-2268, 2016.

10. Kakoty V, Sarathlal KC, Dubey SK, Yang CH and Taliyan R: Neuroprotective effects of trehalose and sodium butyrate on preformed fibrillar form of α-synuclein-induced rat model of Parkinson's disease. ACS Chem Neurosci 12: 2643-2660, 2021.

11. Qing H, Koprich JB, Wang Y, Yu WB, Xiao BG, Brotchie JM and Wang J: Treatment with trehalose prevents behavioral and neurochemical deficits produced in an AAV α-synuclein rat model of Parkinson's disease. Mol Neurobiol 53: 2258-2268, 2016.

12. Ho TT, Warr MR, Adelman ER, Lansinger OM, Flach J, Verovskaya EV, Figueroa ME and Passegué E: Autophagy maintains the metabolism and function of young and old stem cells. Nature 543: 205-210, 2017.

13. Zhou K, Zheng Z, Li Y, Han W, Zhang J, Mao Y, Chen H, Zhang W, Liu M, Xie L, *et al*: TFE3, a potential therapeutic target for Spinal Cord Injury via augmenting autophagy flux and alleviating ER stress. Theranostics 10: 9280-9302, 2020.

14. Williamson SR, Eble JN and Palanisamy N: Sclerosing TFEB rearrangement renal cell carcinoma: A recurring histologic pattern. Hum Pathol 62: 175-179, 2016.

15. Franco-Juárez B, Coronel-Cruz C, Hernández-Ochoa B, Gómez-Manzo S, Cárdenas-Rodríguez N, Arreguin-Espinosa R, Bandala C, Canseco-Ávila LM and Ortega-Cuellar D: TFEB; Beyond its role as an autophagy and lysosomes regulator. Cells 11: 3153, 2022.

16. Chen M, Dai Y, Liu S, Fan Y, Ding Z and Li D: TFEB biology and agonists at a glance. Cells 10: 333, 2021.

17. Nishizaki Y, Yoshizane C, Toshimori Y, Arai N, Akamatsu S, Hanaya T, Arai S, Ikeda M and Kurimoto M: Disaccharide-trehalose inhibits bone resorption in ovariectomized mice. Nutr Res 20: 653-664, 2000.

18. Yoshizane C, Arai N, Arai C, Yamamoto M, Nishizaki Y, Hanaya T, Arai S, Ikeda M and Kurimoto M: Trehalose suppresses osteoclast differentiation in ovariectomized mice: Correlation with decreased in vitro interleukin-6 production by bone marrow cells. Nutr Res 20: 1485-1491, 2000.

19. Komori T: Animal models for osteoporosis. Eur J Pharmacol 759: 287-294, 2015.

20. Xu X, Wang R, Wu R, Yan W, Shi T, Jiang Q and Shi D: Trehalose reduces bone loss in experimental biliary cirrhosis rats via ERK phosphorylation regulation by enhancing autophagosome formation. FASEB J 34: 8402-8415, 2020.

21. Melia TJ, Lystad AH and Simonsen A: Autophagosome biogenesis: From membrane growth to closure. J Cell Biol 219: e202002085, 2020.